

Crosslinker Effect in ETFE Based Radiation Grafted Proton Conducting Membranes

II. Extended Fuel Cell Operation and Degradation Analysis

Hicham Ben youcef ^a, Lorenz Gubler ^{a,*}, Tetsuya Yamaki ^{b,z}, Shinichi Sawada ^b, Selmiye Alkan Gürsel ^{a,**}, Alexander Wokaun ^a, Güenther G. Scherer ^a

^a*Electrochemistry Laboratory, Paul Scherrer Institut, 5232 Villigen PSI, Switzerland*

^b*Japanese Atomic Energy Agency, 1233 Watanuki, Takasaki, Gunma 370-1292, Japan*

*Corresponding author. Tel.: +41-56-3102673; fax: +41-56-3104416. E-mail: Lorenz.gubler@psi.ch

**Present address: Faculty of Engineering and Natural Sciences, Sabancı University, 34956 Istanbul, Turkey

Abstract

In this study the effect of crosslinker (divinylbenzene (DVB)) content on the chemical stability of poly(ethylene-*alt*-tetrafluoroethylene) (ETFE) based membranes using an H₂O₂ solution was carried out. Furthermore, the first long term-testing of single H₂/O₂ cell over 2180h of an MEA assembled using an optimized ETFE-based membrane prepared by radiation-induced grafting of styrene / DVB and subsequent sulfonation with a graft level of 25 % was carried out. The *in situ* MEA properties were characterized over the testing period using auxiliary current-pulse resistance, electrochemical impedance spectroscopy, polarization and H₂ permeation. It is shown that the crosslinking dramatically improves the *ex situ* chemical stability, while no significant trend with the crosslinker content was observed. The performance of the tested MEA exhibits a decay rate of 13 $\mu\text{V}\cdot\text{h}^{-1}$ in voltage over the testing time at 500 mA $\cdot\text{cm}^{-2}$ at 80°C, while the hydrogen permeation shows a steady increase over time. This indicates clearly that to some extent changes in the membrane morphology occur over the operating time. The local *post mortem* analysis of the tested membrane reveals that high degradation was observed in areas adjacent to the O₂ inlet and in other areas nearby.

Keywords: Proton-exchange membrane; Radiation-induced grafting; chemical degradation; ETFE

1. Introduction

The development of cost effective proton exchange membranes to replace the state-of-the-art and expensive perfluorinated membranes (Nafion®, Flemion®, Aciplex®) is one of the main challenges to bring the polymer electrolyte fuel cell (PEFC) technology to a commercial level. The radiation induced grafting technique in combination with low cost base polymer material, either fluorinated or partially fluorinated polymer films, offers several advantages as described elsewhere¹. The radiation induced grafting allows the functionalization of the base material and the introduction of the desired property (proton conductivity). The attractiveness of this technique is based on its versatility and the opportunity to easily control the parameter and tune the desired properties in a wide range, and also the possibility of the use of a wide combination of monomers and materials, respectively.

One of the main research areas in our laboratory at the Paul Scherrer Institut (PSI) is the development of low-cost polymer electrolyte membranes, and promising achievements and results were reached. Radiation-grafted crosslinked membranes based on styrene / divinylbenzene (DVB: crosslinker) and poly (tetrafluoroethylene-*co*-hexafluoropropylene) (FEP) exhibited performance comparable to commercial Nafion®112 membranes and were able to operate over 4000 hours in steady conditions at a temperature of 80°C^{1,2}.

The FEP based membrane was optimized with respect to its performance and chemical stability by adjusting the crosslinker content and graft level. In a study of the effect of DVB on fuel cell performance, the membrane prepared with 10% DVB (in the initial solution) was found to exhibit the best performance³. Recently, partially fluorinated poly (ethylene-*alt*-tetrafluoroethylene) (ETFE) has been revisited as an alternative base polymer film because of its advantages (superior mechanical properties, good resistance to irradiation, higher grafting kinetics) in comparison with the FEP base film⁴. First fuel cell tests based on styrene / DVB grafted ETFE (25 µm) based membranes, prepared using the same conditions as for the optimized FEP-based membranes, were carried out⁵.

The obtained results show clearly the potential of ETFE as base material, but still the system needs to be optimized regarding both key parameters, i.e., the graft level (GL) and the crosslinker content. Subsequently, a detailed study on the influence of grafting parameters and reaction kinetics were performed for styrene onto ETFE for better control and understanding of the system, and differences in kinetics as expected in comparison with the FEP based material were observed⁶. The influence of crosslinker was also investigated and correlation between the DVB content and the *ex situ* relevant properties for fuel cells were established⁷.

The mechanical stability of our grafted films and membranes is a crucial prerequisite in terms of handling, fabrication and durability of the membrane electrode assembly (MEA). The quality control of the membrane before fuel cell testing is an important issue to overcome both the mechanical and swelling stresses due to local dehydration states⁸. An evaluation of the effect of irradiation, graft level and crosslinking were performed, and comparison with the Nafion®112 membrane was established⁹. It was found that the optimization of all these parameters is needed to reduce their negative impact on the elasticity and tensile strength.

Our group not only focused on styrene based grafted membranes, but also on different monomer combinations in order to improve the chemical stability under real fuel cell operating conditions. The use of alternative monomers was recently reported which are prepared with substituted styrene monomers with protected α -position, such as α,β,β -trifluorostyrene derivatives¹⁰ and α -methylstyrene / methacrylonitrile¹¹ to improve the oxidative stability of our membranes. In addition, the durability test of our membranes is one major focus which is an important tool for evaluating the membrane and the MEAs. Furthermore, new methods for rapid aging are also developed to evaluate the membrane stability and the chemical and physical degradation occurring under aggressive conditions (OCV, high pressure, r.h. cycling)¹².

The influence of the graft level and degree of crosslinking on the *ex situ* and *in situ* properties of the grafted ETFE-based membranes was investigated in detail^{5,13}. Based on these earlier findings, increasing GL was pointed out to lead to more brittle membranes, while lower GL does not afford good conductivities. The optimal GL was identified between 24 and 30 %, where the mechanical integrity, conductivity and performance of the grafted membranes are well-balanced⁵. Moreover, it was found that the water uptake and the conductivity were negatively affected by the increase of the crosslinker content. In addition, the increase of the crosslinking in the membrane induces an increase of their brittleness and *in situ* ohmic resistance. The fuel cell test of the membrane using 5% DVB in the initial grafting solution was found to exhibit the maximum performance and was identified as optimal concentration¹³.

For the present study, the optimized crosslinked ETFE-based membrane was prepared with a graft level of 25 %. Furthermore, the effective DVB content of the grafted membrane was determined by FTIR, which was pointed out to be different from the concentration in the initial grafting solution⁷. The obtained membrane was then characterized for its relevant fuel cell properties (IEC, water uptake, conductivity, mechanical properties) and an MEA was prepared and a durability test carried started. The MEA was intermittently characterized over the testing period and the *in situ* properties were determined using auxiliary current-pulse resistance, electrochemical impedance spectroscopy, polarization curves and H₂ permeation. Furthermore, a local *post mortem* analysis using FTIR was performed to produce a degradation map over the active area.

2. Experimental

2.1. Membrane preparation

Radiation grafted membranes based on Tefzel® ETFE 100LZ film (DuPont, Circleville, OH, USA) were prepared using the procedure reported earlier⁷. A monomer solution composed of styrene (purum grade; Fluka) and DVB (technical grade, ~80%, mixture with isomers 3- and 4-ethylvinylbenzene; Fluka) with varying styrene : DVB ratio (v/v) was prepared. This monomer mixture was added to the solvent prepared with isopropanol (analytical grade; Fisher Scientific) and water at a ratio of 11:5 (v/v).

2.2. Mechanical properties

The mechanical properties of the membranes based on ETFE were measured by Universal Testing Machine (Zwick Roell Z005) with a maximum test load of 5 kN. The measurements were performed at a cross head speed of 100 mm min⁻¹. Details of the procedure can be found in our earlier contribution⁹.

2.3. Ion exchange capacity, water uptake and conductivity

The sulfonation of the grafted films to yield proton conducting membranes, and methods used for *ex situ* characterization (ion exchange capacity, water uptake, proton conductivity) are reported elsewhere⁵.

2.4 Single fuel cell testing and in situ characterization

The ETFE-based membrane with a graft level of 25.2 % and crosslinked using 5% DVB (v/v) monomer in the grafting solution was hotpressed together with ELAT® electrodes (type LT140EWSI, E-TEK / BASF Fuel Cell, Inc.) with a platinum loading of 0.5 mg Pt cm⁻² at 110 °C / 15 kN / 180 s to form a membrane electrode assembly (MEA). The electrochemical characterization (polarization curves, impedance spectroscopy, H₂ permeation...) and the description of the used procedure are described in detail in our first part contribution¹³.

2.4 Chemical degradation

Membrane samples were dried in the oven under vacuum, then weighed and immersed in ultra pure water overnight (water-equilibration step). Subsequently, the samples were inserted into glass beakers containing a 3 % H₂O₂ aqueous solution and treated for different periods of time at 60 °C. The samples were then removed, immersed again in pure water and agitated for more than 24 h. The final step was to wash them in water and dry them in the oven under vacuum overnight, after which they were weighed for the second time¹⁴.

The relative weight loss can be calculated by the following equation:

$$\text{Weight loss (\%)} = \frac{W_d(t)}{W_d(0)} \times 100$$

$W_d(0)$: weight of the dry membrane at $t = 0$.

$W_d(t)$: weight of the dry membrane after H_2O_2 treatment.

2.5 Post mortem analysis

After stopping the fuel cell test, the MEA was disassembled and the membrane exchanged into salt form (K^+) by immersing in 0.5 M KCl overnight and then dried at 60°C for at least 16 h. A *post mortem* analysis by FTIR was performed in the non-active and active area of the tested membrane by the use of a metallic slit mask (rectangular aperture 0.5 cm x 1.9 cm). The area of the aromatic peak appearing at 1494 cm^{-1} assigned to styrene was measured to determine the extent of degradation as follows:

$$\text{Degradation (\%)} = \frac{\text{peak area (tested)} - \text{peak area (untested)}}{\text{peak area (untested)}} \times 100$$

3. Results and Discussion

3.1. Ex situ relevant properties of the ETFE-based membrane

Based on our previous study on the effect of crosslinking, graft level and irradiation dose on different *ex situ* properties (thermal stability, mechanical stability, conductivity, etc.), an optimized membrane based on radiation grafted styrene / DVB onto ETFE was defined. Furthermore, an investigation of the effect of crosslinker content on the *in situ* properties (performance, resistance, interface, etc.) of these membranes was carried out¹³. It was found that the maximum performance were reached using the membrane based on 5% DVB (v/v). For the present investigation, a grafted ETFE-based film with a 25.2% graft level was sulfonated to introduce the ion exchange sites. The thickness of the obtained membrane and the effective extent of crosslinking (DVB) were then determined by FTIR (TABLE I). The obtained value of the DVB / styrene molar ratio in the membrane is significantly (~50%) higher than the value in the initial grafting solution. Furthermore, this result is in accordance with the previous observation on the grafting of styrene / DVB onto ETFE-based films⁷. The DVB was found to be more reactive than the styrene due to its double reactive functions (double bond) and to be highly incorporated close to the surface in comparison to the entire bulk of the grafted film (ATR vs. transmission measurements). Moreover, the thickness of the resulting grafted ETFE-based membrane measured in the wet form is rather low compared to that of Nafion®112.

TABLE I. Characteristic of the ETFE-based membranes and measured composition by FTIR.

Membrane	GL	Molar ratio (DVB/St)		Thickness
		initial solution	initial solution	
	[%wt]	[%]	[%]	[μm]
ETFE-25	25.2	4.3 +/- 0.0	6.7 +/- 0.1	34.0 +/- 0.6
Nafion®112	-	-	-	58.0 +/- 3.0

* Thickness measured for the membrane in liquid water equilibrated state.

The mechanical properties of the resulting membrane converted to salt form were evaluated in dry state regarding both direction, machining (MD) and transverse direction (TD) (machining is referring to the extrusion direction of the produced roll) (TABLE II). The crosslinking and the graft level were previously pointed out to play a determining role in the resulting mechanical properties of the radiation grafted ETFE based membrane. The study of the influence of the crosslinker concentration and graft level on the mechanical properties reveals that the most affected parameter is the elongation at break. Indeed, the brittleness of the ETFE-based grafted films and membranes increase drastically with the increase of the graft level and the crosslinker concentration⁹. In both type of membranes, the elongation at break and Young modulus of the membrane in the TD are higher than the values obtained in the MD, whereas the inverse is observed for the tensile strength (as expected from the orientation during the processing of the base film). The ETFE-based membrane shows higher elongation at break and Young modulus in both directions than the Nafion®112. Furthermore, the tensile strength of the ETFE-based membrane is higher in the transverse direction, while comparable values were measured in the machining direction. So far, no mechanical parameters were specified to yield better mechanical stability in a real fuel cell test environment. Nevertheless, obviously as much as we can increase the extensibility and the strength of the membrane, the better will be the mechanical integrity in a much more severe environment. Furthermore, dealing with radiation grafted based membranes it was found that the less we irradiate, graft and crosslink, the better are the mechanical properties. Then the most important aspect is to adjust all these parameter in a balanced way to obtain better compromise between *ex situ* properties, performance and durability. More work is addressed currently to investigate in detail the tensile properties under fuel cell relevant conditions, i.e., at higher temperature and relative humidity.

TABLE II. Mechanical properties of the ETFE-based membranes and Nafion®112 in both machining (MD) and transverse direction (TD).

Membrane	Direction	Elongation at	Tensile	Young
		break	strength	modulus
		[%]	[MPa]	[MPa]
ETFE-25	MD	114 +/- 15	50 +/- 2	820 +/- 47
	TD	139 +/- 27	46 +/- 2	844 +/- 34
Nafion®112	MD	87.4 +/- 8	50 +/- 5	567 +/- 22
	TD	126 +/- 14	38 +/- 2	575 +/- 25

The *ex situ* properties (IEC, water uptake, conductivity and hydration number) are the most important data for fuel cell performance. The representative results for the grafted ETFE-based membrane were determined and compared to the values of Nafion®112 (TABLE III)⁵. The Nafion®112 shows higher water content and conductivity than the ETFE-based membrane, while the value of IEC is lower (mass based values). Furthermore, the values of IEC, taking into account the difference in densities between both types of membranes, were evaluated and values of 2.4 meq.cm⁻³ and 1.6 meq.cm⁻³ for ETFE grafted membrane and for Nafion®112, respectively, were determined¹³. The observed difference in conductivity is maybe due to the higher volumetric IEC of the grafted ETFE based membrane compared to Nafion®112. Furthermore, the lower water content in the ETFE based membrane can be easily understood from the crosslinker content, which was determined previously by FTIR. It is important to note here that Nafion®112 is not a crosslinked membrane and comparable water content and conductivity was observed with the uncrosslinked ETFE-based membrane. Furthermore, comparison of these values with the FEP based membranes was already discussed and can be found elsewhere¹³.

TABLE III. Measured value of IEC, water uptake, hydration number and conductivity of the ETFE-based membranes compared with the values of Nafion®112.

Membrane	IEC	Conductivity *	Water uptake *	Hydration number
	[meq.g ⁻¹]	[mS.cm ⁻¹]	[%wt]	[n(H ₂ O) /n(SO ₃)]
ETFE-25	1.6 +/- 0.1	64 +/- 3	20.6 +/- 0.6	7.0 +/- 0.5
Nafion®112	0.9 +/- 0.1	82 +/- 6	33.5 +/- 1.8	18.0 +/- 0.9

* Measurements were performed in fully swollen state at room temperature.

3.2. *Ex situ* chemical degradation

The interaction of the H_2/O_2 with the platinum during the fuel cell operating conditions results in creation of different peroxyradicals or hydroperoxyradicals (OH^\bullet , HOO^\bullet), which are an aggressive degrading agent for the membranes^{15,16}. One method to pre-evaluate the chemical stability of our membrane was to apply a moderate accelerated test, where an H_2O_2 solution is used instead of the severe Fenton reagent, which leads to very fast degradation kinetics¹⁴.

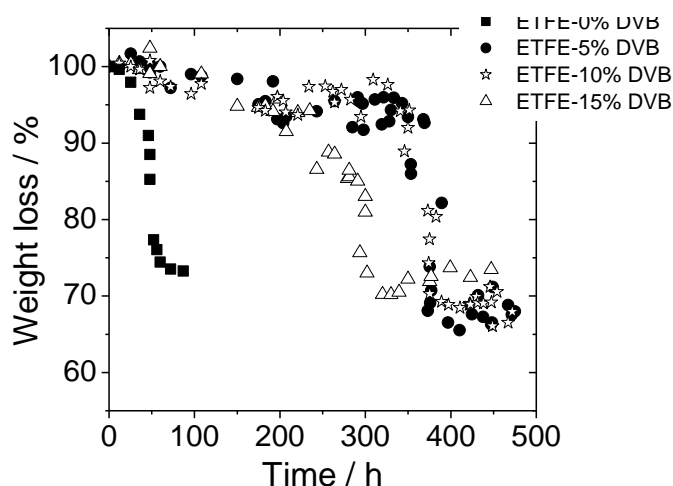


Figure 1. *Ex situ* chemical degradation of ETFE-based membranes (GL~25%) with different DVB content (in the initial grafting solution) in 3 % H_2O_2 at 60°C.

The influence of the DVB concentration on the chemical stability of the ETFE based membranes with fixed graft level of ~25% was studied. Various membranes based on ETFE with different DVB content (0, 5, 10 and 15% DVB in the initial grafting solution) were prepared and tested for their *ex situ* chemical stability by immersing them in a solution of H_2O_2 at 60°C. The IEC of all membranes was determined prior to the test and the same value of around 1.7 meq g^{-1} was measured. The chemical degradation of these ETFE-based membranes was measured and the evolution of the weight loss is depicted in **Figure 1**. The weight loss threshold decrease was taken as the onset of the degradation time and was used for the comparison of the chemical stability. The membrane weight started to decrease for all samples and then reached a constant value assumed to be the remaining base polymer of ETFE, Thus confirmed by the calculated values of the samples weight based on the IEC and GL data. The weight loss is most likely due to polymer chain scission occurring in the membranes, which are subsequently washed out¹⁴. It was stated previously that the existence of (OH^\bullet , HOO^\bullet) radicals in the solution may provoke an attack on the styrene unit, leading to the formation of a benzyl radical and, eventually, scission of the C-C bond on the polymer chain¹⁶. Study of the decomposition products in the produced water from the fuel cell based on styrene grafted FEP membranes was performed using a high-

pressure liquid chromatograph (HPLC), revealing mainly the formation of monomeric residues. Furthermore, a Raman investigation of styrene based grafted PVDF membranes shows a loss of the poly(styrene sulfonic acid) groups after fuel cell tests^{15,17}. Comparing the obtained results, the first main observation is that crosslinking induces generally an increase in the chemical stability of the ETFE-based membrane. Furthermore, the highly crosslinked membrane (15% DVB) was found to possess a lower stability, even though the crosslinker concentration was highest, whereas the 5% and 10% DVB based membranes shows similar stability. Several factors may play a significant role in that observed behavior. In fact, higher crosslinker concentration in the grafting solution induces an increase in the number of pending double-bonds in the grafted membranes as observed by FTIR, which affect the efficiency of the DVB as crosslinker²⁰. The higher crosslinking may also produce higher number of chain ends, and consequently the probability to form polymer branches with lower molecular weight (lower chain-length), which are easily degraded, in the membrane is higher.

3.3. Fuel cell durability test

After assembling the grafted ETFE-based membrane (5% DVB) into the fuel cell, an MEA durability test was performed at a constant current density of 500 mA.cm^{-2} . The collected cell performance and the measured ohmic resistance by the pulse method of the membranes over the testing time are shown in **Figure 2**. The evaluated drop in voltage after 1100 h was around 11 mV, whereas this value was of about 21 mV at the end of the test (2180 h). Moreover, the fitting of the voltage over the testing time shows a voltage decay rate of about $13 \text{ } \mu\text{V.h}^{-1}$. Looking more closely at the history plot, the voltage shows two different decay rates, the first occurring from the beginning of the test up to 1100h with a value of $7 \text{ } \mu\text{V.h}^{-1}$ whereas a value of $23 \text{ } \mu\text{V.h}^{-1}$ was determined for the second (from 1100 h up to 2100 h). Concerning the ohmic resistance of the tested MEA, no change was noticed for the pulse measured ohmic resistance up to 1100 h, while an increase of 6 % was observed up to 1508 h, and then a further increase of 7 % was measured up to 2100 h. The membrane resistance increases from initially $94.5 \text{ m}\Omega.\text{cm}^2$ to $\sim 100 \text{ m}\Omega.\text{cm}^2$ after 1100 h, and then reaches a value of $\sim 106 \text{ m}\Omega.\text{cm}^2$ at the end of test. Both stepwise changes in resistance were observed after restarting the cell, which may indicate the adverse effect of start-stop cycles and their association with degradation phenomena in our system^{2,15}.

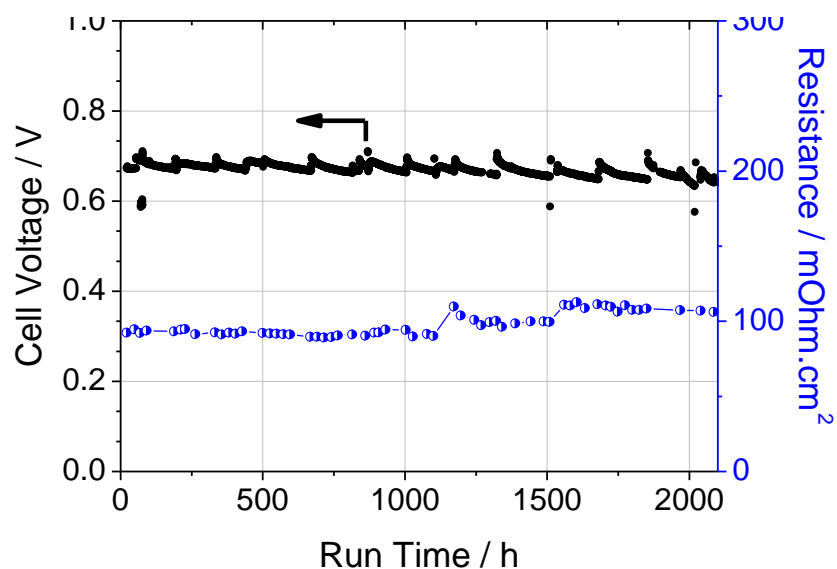


Figure 2. Single cell durability test using a radiation grafted membrane based on ETFE (5% DVB) @500mA.cm⁻², cell temperature 80°C; H₂/O₂ at a stoichiometry of 1.5/1.5.

The fuel cell performance of the MEA was measured and the polarization curves obtained over the testing time are shown (**Figure 3**). The performance of the ETFE-based membrane and the Nafion®112 after about 500h of operating time shows similar results. However, the measured pulse ohmic resistance of the Nafion®112 was slightly higher, even showing a marked increase at high current densities starting from 1250 mA.cm⁻². This may be the result of a stronger dehydration by the effect of electroosmotic drag on the anode side, which induces an increase in the area resistance. Moreover, the difference of membrane microstructure, the water transport mechanism and the membrane-electrode interface may play non-negligible role here^{5,18}. Up to 1174 h of time on test, no significant change in the voltage was observed, yet at 1968 h a slight decrease at high current densities was measured. The ohmic resistance does not show any significant change up to 1174h, where after an increase leading the ETFE-based membrane to reach the same values to those of the Nafion®112 was observed after 1968h. However, the ETFE-based membrane does not show any marked increase over the testing time in resistance at high current densities as observed for the Nafion®112.

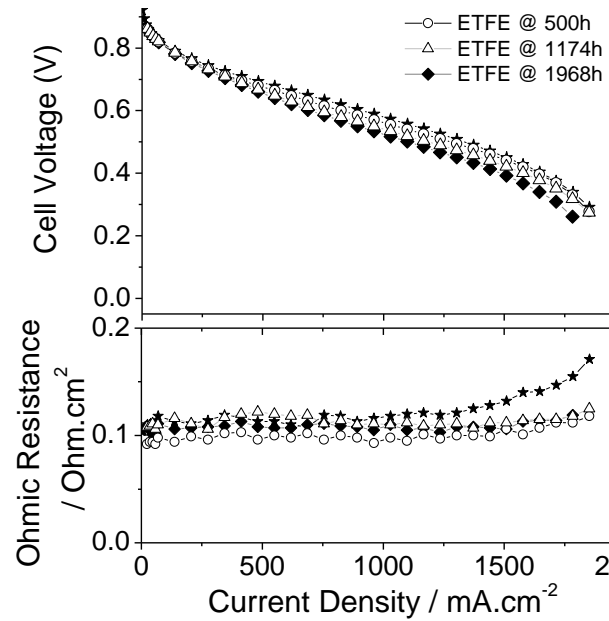


Figure 3. Polarization curves of the ETFE-based membrane over the testing-time at $500 \text{ mA}\cdot\text{cm}^{-2}$, cell temperature 80°C ; H_2/O_2 at a stoichiometry of 1.5/1.5.

The extracted open circuit voltage (OCV) values at various operating time for the MEA are shown (**Figure 4**). The first general observation is that the OCV values shows two distinct levels. The first one starts from the beginning up to 815 h, while the second one starts from 1004 h until the end of test. Moreover, the OCV slightly decreased from 0.924 V measured at 68 h to a value of 0.920 V at 188 h, which is assumed to be a consequence of the time needed for the cell and to the interface of the MEA to operate in equilibrium. The observed trend for the OCV correlates with the measured changes in the decay rates of the cell voltage.

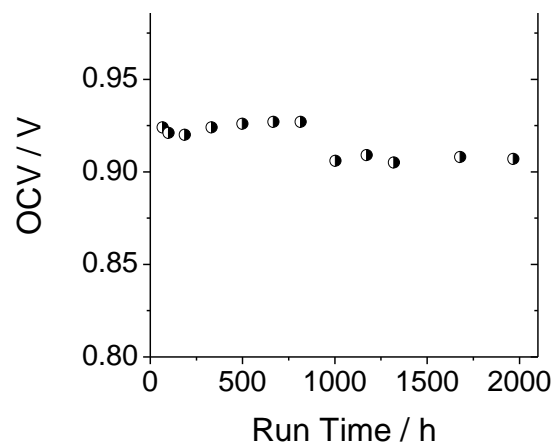


Figure 4. Evolution of the OCV value over the testing time at $500 \text{ mA}\cdot\text{cm}^{-2}$, cell temperature 80°C ; H_2/O_2 at a stoichiometry of 1.5/1.5.

In order to resolve the different losses occurring within the MEA, electrochemical impedance spectroscopy was performed intermittently over the testing period (**Figure 5**). From the electrochemical impedance spectra, the ohmic resistance was determined from the intersection of the impedance spectrum with the real axis at the high frequency end, whereas the polarization resistance was obtained by subtracting the ohmic resistance from the resistance value at the intersection of the spectrum with the real axis at the low frequency end.

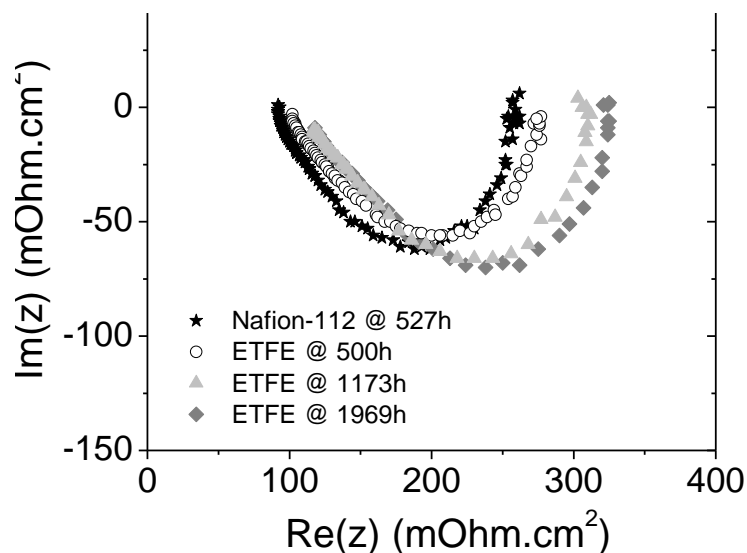


Figure 5. Ac impedance spectra recorded at a DC current density of 500 mA.cm^{-2} after different run time shown in Nyquist representation (frequency range: 0.1 Hz – 25 kHz).

The first observation is that the Nafion®112 based MEA exhibits both lower ohmic and polarization resistance in comparison with the MEA with grafted ETFE membrane. The higher interfacial resistance (polarization resistance) in the case of the ETFE-based membrane was already pointed out to be mainly due to the lower compatibility of these grafted membranes to the Nafion® ionomer used in the catalyst layer¹³. The resistance values extracted from the ac impedance spectra are depicted in **Figure 6**. The ohmic resistance does not show any change up to 800 h, whereas a slight increase of ~4% after 1200 h was observed. The polarization resistance of the ETFE based membrane decreases slightly up to 500 h and then increases after 800 h and 1200 h, then no significant change is observed after this period. The observed slight decrease in the polarization resistance up to 500 h is most probably due to the improvement of the membrane-electrode interface which needs an equilibrating time to establish. The extracted data of both resistances shows an increase after 1200 h, which is a sign of deterioration of the MEA. Moreover, the obtained results are in accordance with the observed loss in the OCV at 1000 h, owing to the sensitivity of the membrane to start-stop events. This may indicate that at some point an irreversible and local drying of the membrane occurs. We should note here that the absolute

ohmic resistance values determined by EIS are slightly higher than the values measured by the current-pulse method due to the effect of cable inductance during measurements at high frequency.

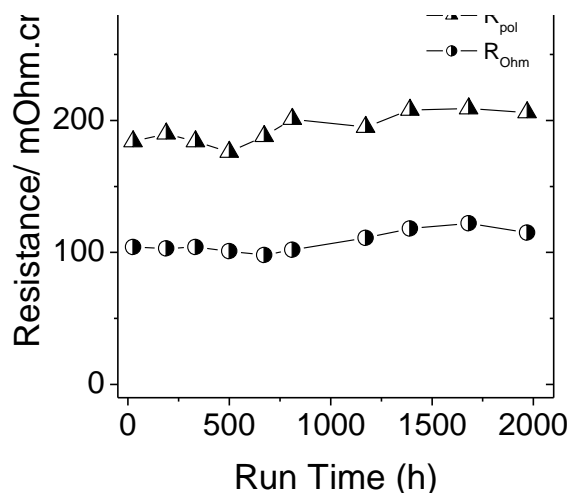


Figure 6. Extracted ohmic (R_{Ω}) and polarization resistance (R_{pol}) from the EIS-spectra at $500 \text{ mA}\cdot\text{cm}^{-2}$.

It was also important to investigate the H_2 crossover of the ETFE-based grafted membrane over the testing time due to the close relationship existing with the rate of chemical degradation and the possible changes in the morphology of the membrane and its mechanical integrity (Figure 7). The hydrogen crossover shows a steady increase with increasing testing time up to 2000 h, and a corresponding H_2 permeation rate of $> 10 \text{ ml min}^{-1}$ was observed at the end of test after 2180h. It can be noticed here that the evolution of the H_2 crossover shows different changes over the testing time with respect to the initial value, i.e., an increase of 18% is observed up to 500 h while a decrease of 6% was determined after 670 h, then a quasi-linear increase arise up to 1681 h, where the variation was 78%, and finally the third increase is determined at 2020 h, where the H_2 crossover variation was 152%. These results indicate clearly that to some extent changes in the membrane morphology and integrity occur over the operating time, in accordance with other measured *in situ* parameters (performance, ohmic and polarization resistances). Dealing with a grafted membrane, the water management and the hydration-dehydration states become crucial issues in the durability and mechanical integrity. Furthermore, the water is known to play the role of a plasticizer, allowing more mobility of the chains, which means also more change in the local morphology, the mechanical stress between amorphous and crystalline zones, and the possible thinning of the membrane, which may result in the observed increase in gas permeation. The correlation of this result with the extent of degradation occurring in the membrane will be discussed in the next section dedicated to the *post mortem* analysis.

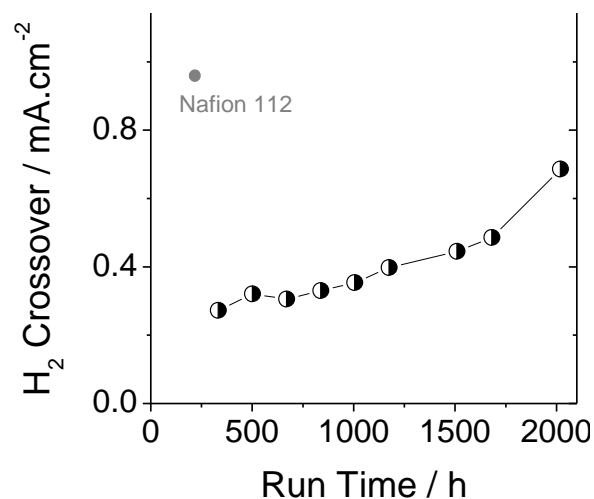


Figure 7. Hydrogen crossover measured in H₂/N₂ mode at 80°C.

3.4. Post mortem analysis

The cell was disassembled and the membrane was separated from the electrode by immersing the MEA in water and use of ultrasound (Fig.8). The first observation is that the membrane shows an entire crack in the edge zone (the border between the active and non-active area). In fact, pinhole formation was suspected from the sudden drop of performances after 2181 h and the measured H₂ crossover (> 10 ml.min⁻¹).

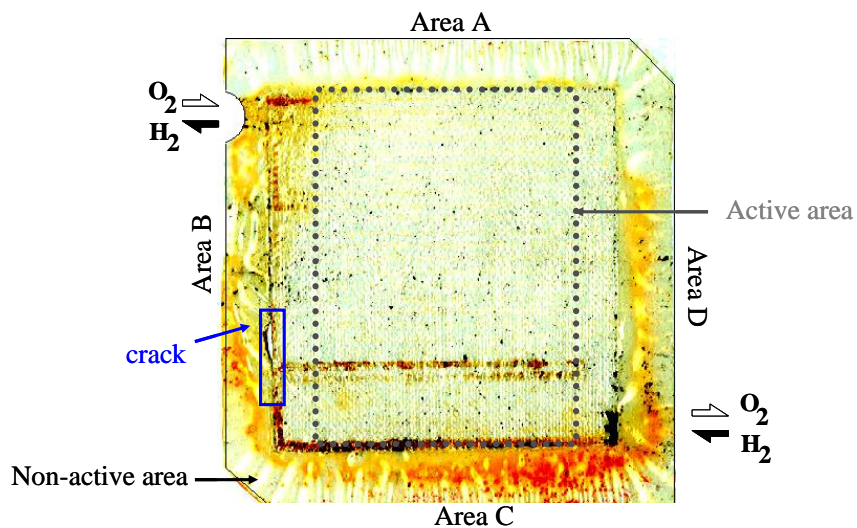


Figure 8. Scanned image (contrast enhanced) of the membrane disassembled from the MEA after 2180h on test.

To begin with, it was of importance to evaluate the extent of degradation in the non-active area (Area A, B, C and D as shown in Figure 8), where selected points of the membrane (exchanged into K^+ salt form and dried) were measured by FTIR (TABLE IV). The area B shows marked degradation in comparison with the other non-active zones, while both areas A and D shows similar trends and less loss was observed. Interesting results were determined for the area near the hydrogen inlet of the tested membrane (area C), where the minimum degradation occurred. These results are somewhat surprising, since previously this area (non-active) was stated as a reference for the evaluation of the degradation, since no deterioration was observed on it²¹. Furthermore, the marked difference in the extent of degradation between the Area B and the rest of the non-active area is not yet understood. The high degradation in zone B, where the crack was located and formed, raises several questions about the extent of external gas crossover (leak tightness) of the MEA and the efficiency of the used gasket. Furthermore, the high chemical degradation also assumes propagation of peroxides in these areas or existence of other sub-phenomenon which occurs in the presence of some potential contaminants and H_2/O_2 .

TABLE IV. Measured degradation in the non-active area for the Area A, B, C and D.

	Area (A)	Area (B)	Area (C)	Area (D)
% Degradation	38 +/- 14	82 +/- 14	10 +/- 6	38 +/- 10

The dried and exchanged membrane (K^+ form) was then characterized by FTIR to determine the extent of degradation in the active area in all channel/land areas (53 channels and lands in total). Furthermore, to map the degradation on the active area, 7 points in lateral direction were measured for each channel and land, and the obtained degradation map is presented in Figure 8. If we consider the overall area, we find that the extent of degradation in the channels was higher than in the lands of the active area. In fact, the extent of degradation in the channels was averaged to be 18%, while the value in the lands was about 13%. Furthermore, the obtained results do not show any significant difference or clear trend between the channels and lands when comparing only the slightly degraded zone, where the values were 11.6% and 11.7% in the channels and lands, respectively. The averages of degradation in the highly and the slightly degraded zone were determined regardless of the channel and land area in the membrane and correspond, respectively, to 51% and 12%. The higher degradation features were observed in the channels and lands in the first serpentine (Channel-53 and land-52) located near the O_2 entrance, between the channel-41 and -43) and in the channel-31. The observed feature brings more questions than answers, about the how and why the degradation occurs at these positions and the possible formation of small pinholes. The unexpected results were on the one hand the absence of any degradation gradient between the affected channels and lands, in addition to the lack of correlation between the highly degraded active zone and the crack location in the membrane. Consequently, the crack forming in our

case may be assumed to be mostly due to mechanical failure of the membrane due to stress in this area between the hydrated active and non-hydrated inactive area where high degradation was measured.

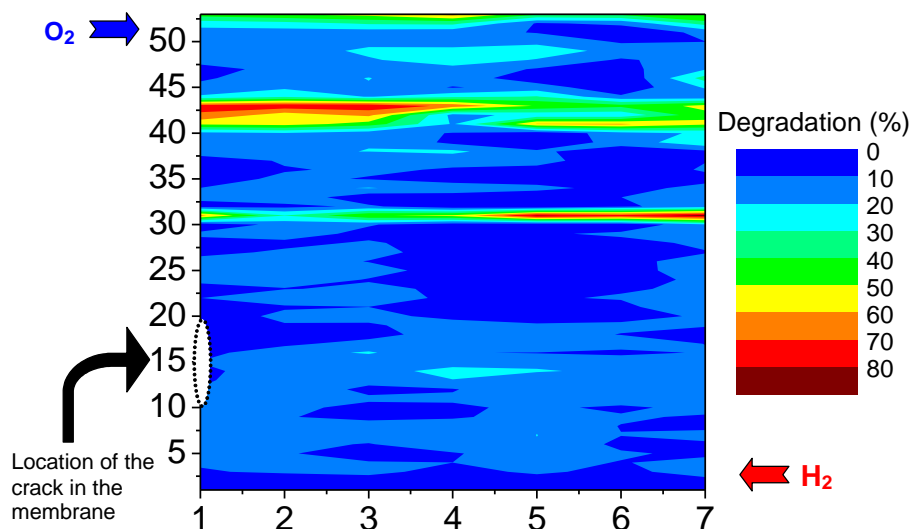


Figure 8. Map of the extent of degradation of the ETFE based membrane located in the active area.

4. Conclusion

A fuel cell membrane based on optimized styrene/DVB grafted ETFE membrane with a graft level of 25% was characterized for its *ex situ* relevant fuel cell properties (IEC, water uptake, conductivity and mechanical properties). The conductivity of the grafted membrane was shown to be slightly lower than that of Nafion®112, while the water uptake shows an opposite trend, which is mainly attributed to the different densities and the effect of crosslinking and reduced free volume available within the polymer structure. Furthermore, the ETFE-based membrane shows slightly superior mechanical properties in terms of elongation at break and tensile strength.

A durability test with the optimized ETFE-based membrane was performed in a single fuel cell over a testing period of 2180 h. The MEA shows two regimes in cell voltage loss up to 2100 h, where a sudden drop was observed after 2180h due to crack formation in the membrane. Moreover, the tested cell shows comparable performance to that of Nafion®112 and only slight decrease at high current densities was observed up to 2000 h. The *post mortem* analysis reveals that the high extent of degradation was more located near to the O₂ inlet, and the membrane areas associated with flow field channels were more affected than the respective land areas. It was found that degradation occurred in the non-active area to different extent, depending on the location of the measured points. Moreover, the crack forming observed in the membrane was located at the boundary between the area which shows low degraded active area and the highly degraded non-active area.

Consequently, the MEA at the area between the active and non-active zone, even though covered by the gasket, was subjected to stress due to hydration-dehydration phenomena.

Acknowledgement

The authors wish to thank Manuel Arcaro, Friederike Geiger and Christian Marmy for technical support. Funding by the Swiss Federal Office of Energy (SFOE) is gratefully acknowledged.

References

1. L. Gubler, S.A. Gürsel, G.G. Scherer, *Fuel Cells*, 5, 317 (2005).
2. L. Gubler, H. Kuhn, T.J. Schmidt, G.G. Scherer, H.P. Brack, K. Simbeck, , *Fuel Cells*, 4, 196 (2004).
3. T.J Schmidt, K. Simbeck, G.G. Scherer, *J. Electrochem. Soc.*, 152, A93 (2005).
4. H. P. Brack, F. N. Büchi, J. Huslage, M. Rota, G. G. Scherer, *ACS symp.*, 744, 174 (2000).
5. L. Gubler, N. Prost, S.A. Gürsel, G.G. Scherer, *Solid State Ionics*, 176, 2849 (2005).
6. S. Alkan Gürsel, H. Ben youcef, A. Wokaun, G. G. Scherer, *Nucl. Instr. and Meth. in Phys. Res. B*, 265, 198 (2007).
7. H. Ben youcef, S. Alkan Gürsel, A. Wokaun, G. G. Scherer, *J. Memb. Sci.*, 311, 208 (2008).
8. A. B. LaConti, M. Hamdan, R. C. McDonald, in *Handbook of Fuel Cells-Fundamentals, Technology and Applications: Vol. 3*, John Wiley & Sons Ltd., (2003) ISBN: 0-471-49926-9.
9. H. Ben youcef, S. Alkan Gürsel, A. Buisson, A. Wokaun, G. G. Scherer, (to be submitted).
10. S. Alkan Gürsel, Z. Yang, B. Choudhury, M.G. Roelofs, G.G. Scherer, *J. Electrochem. Soc.*, 53, A1964 (2006).
11. L. Gubler, M. Slaski, A. Wokaun, G.G. Scherer, *Electrochem. Commun.*, 8, 1215 (2006).
12. L. Gubler, M. Schisslbauer, G.G. Scherer, *PSI Electrochemistry Annual Report*, ISSN:1661-5379, (2007).
13. L. Gubler, H. Ben youcef, S. Alkan-Gürsel, A. Wokaun, G.G. Scherer, *J. Electrochem. Soc.* , (submitted).
14. T. Yamaki, J. Tsukada, M. Asano, R. Katakai, M. Yoshida, *J. Fuel Cell Science and Technology*, 4, 56 (2007).
15. B. Mattsson, H. Ericson, L. M. Torell, F. Sundholm, *Electrochimica Acta*, 45, 1405 (2000).
16. G. Hübner, E. Roduner, *J. Mater. Chem.*, 9, 409 (1999).
17. F. N. Büchi, B. Gupta, O. Haas, G. G. Scherer, *Electrochimica. Acta*, 40, 345 (1995).

18. T. J. Schmidt, J. Baurmeister, *J. Power Sources*, 176, 428 (2008).
19. F. N. Büchi, G. G. Scherer, *J. Electrochem. Soc.*, 148, A183 (2001).
20. H. -P. Brack, D. Fischer, G. Peter, M. Slaski, G. G. Scherer G. G. Scherer, *J. polym. sci.:Part A:Polym. chem.*, 42, 59 (2003).
21. M. Slaski, L. Gubler, G.G. Scherer, A. Wokaun, *PSI Scientific Report*, ISSN 1423-7342, (2004).